AIAA 80-0724R

Minimum Mass Sizing of a Large Low-Aspect Ratio Airframe for Flutter-Free Performance

William H. Greene* and Jaroslaw Sobieszczanski-Sobieski†
NASA Langley Research Center, Hampton, Va.

A procedure for sizing an airframe for flutter-free performance is demonstrated on a large, flexible supersonic transport aircraft. The procedure is based on using a two-level reduced basis or modal technique for reducing the computational cost of performing the repetitive flutter analyses. The supersonic transport aircraft exhibits complex dynamic behavior, has a well-known flutter problem and requires a large finite-element model to predict the vibratory and flutter response. Flutter-free designs are produced with small mass increases relative to the wing structural weight and aircraft payload. In view of the ability of the resizing procedure to handle this supersonic transport configuration, it seems likely that the method could be used for many other aircraft.

Nomenclature

$[A]$, $[\tilde{A}]$, $[\bar{A}]$	= matrix of unsteady aerodynamic force coefficients and generalized aerodynamic force matrices of orders m_1 and m_2, respectively
G	= flutter constraint
g_{max}	= value of the assumed structural damping
g_{ref}	= reference value of damping
$[K]$, $[\tilde{K}]$, $[\bar{K}]$	= structural stiffness matrix and matrices of generalized stiffness coefficients of orders m_1 and m_2, respectively
m_0	= number of degrees of freedom in the finite-element model
m_1	= number of vibration modes used in reducing the order of the approximate vibration problem
m_2	= number of approximate vibration modes used in reducing the order of the flutter eigenvalue problem
n	= number of design variables
q	= dynamic pressure, Eq. (8)
$[q]$	= $m_1 \times m_2$ matrix of approximate, generalized vibration mode shapes for the modified structure
$[u]$	= $m_2 \times m_2$ matrix of generalized flutter mode shapes
V	= flutter speed
V_{req}	= required flutter speed
v_i	= value of the ith design variable
$[\Delta]$	= $m_0 \times m_0$ matrix of natural vibration modes
$[\delta]$	= $m_1 \times m_1$ matrix of generalized vibration mode shapes
Ω	= diagonal matrix of vibration frequencies
ω	= diagonal matrix of flutter frequencies
$[\phi]$	= $m_0 \times m_1$ matrix of vibration mode shapes generated at the beginning of each cycle

Presented as Paper 80-0724 at the AIAA/ASME/ASCE/AHS 21st Structures, Structural Dynamics and Materials Conference, Seattle, Wash., May 12-14, 1980; submitted July 31, 1980; revision received July 10, 1981.

*Aerospace Engineer, Structural Concepts Branch, Structures and Dynamics Division. Member AIAA.

†Head, Multidisciplinary Analysis and Optimization Branch, Loads and Aeroelasticity Division. Associate Fellow AIAA.

Introduction

THE difficulties in developing efficient techniques for automated design of flutter-free aircraft stem from the complexity of the flutter phenomenon and the computational cost associated with predicting this behavior. As modifications are made to the structure, the flutter behavior may change in a complex and highly nonlinear way. Also, if the constraints against flutter are formulated simply as a requirement that the lowest flutter speed exceed some required value, the values of the constraints may be discontinuous functions of the structural changes. A review of the work in this area up until 1974 is presented in Ref. 1.

Solutions to the problems of the nonlinear, discontinuous behavior of the flutter constraints and the high computational cost have been proposed. Reference 2 formulates the flutter constraints, considering all critical points for all flutter modes. This insures that the flutter constraints will not have discontinuous values during the design process. However, formulating the constraints in this way may increase the cost of the repetitive flutter calculations. To reduce the high cost of repetitive calculations, an approximate analysis technique utilizing a reduced basis method is proposed in Ref. 3. This technique provides a means for rapidly recalculating the flutter constraints during the design process. The continuous constraint formulation and this approximate analysis method are coupled in the flutter resizing system described in Ref. 3. The performance of the system was demonstrated in Ref. 3 by application to a relatively simple problem—that of a clipped delta wing. However, these techniques have not been applied to a problem with complex dynamic behavior which requires a large mathematical model to predict flutter.

The purpose of the present study is to apply the flutter redesign techniques described in Ref. 3 to this difficult problem of an arrow-wing transport. The difficulties of applying automated design techniques for flutter elimination to a similar supersonic transport are discussed in Ref. 4. Specifically, the objective is to take an airframe sized for strength considerations only and produce a flutter-free design while minimizing the mass added to the airframe. The geometrical and structural complexities of this airframe suggest that a method shown successful for this case is likely to be general enough to apply to many other airframe configurations.

Baseline Analytical Model

The finite-element model of the arrow-wing supersonic transport configuration used in this study is described in Ref. 5. Its basic characteristics are given in this section. The flutter resizing procedure is applied to an airframe that has already been sized to satisfy static load requirements. The static loading cases and the procedure for sizing the airframe for strength criteria are described in Refs. 5 and 6.

The wing is built of corrugated web spars and ribs with caps supporting honeycomb sandwich covers. Conventional stringer-skin-frame construction is used in the fuselage. Titanium is used throughout the primary structure.

Finite-Element Model

The finite-element model representation of this configuration and the types of construction are shown in Fig. 1. In the finite-element model, the wing covers are simulated by membrane elements, the spar and rib webs by shear panels, and the caps by rod elements. Beam elements are used to represent the engines, engine mounts, and supports for leading- and trailing-edge devices. Plate elements are used to model the vertical fins and horizontal stabilizers. Nonstructural components are represented by appropriate lumped and distributed masses. For computational economy, the fuselage model is simplified to a rectangular cross-section thin-walled box with a bending stiffness and mass distribution equivalent to the fuselage. This simplification is consistent with the study's emphasis on the primary wing structure; only elements in the wing structure are resized. The resulting half airplane finite-element model has 746 grid points, 2141 degrees of freedom, and 2369 finite elements.

Sizing for Strength Requirements

From the multitude of loading cases considered in the design of airframes, three cases were selected for use in the strength sizing. The cruise case defines the jig shape and accounts approximately for fatigue, the maneuver case generates the largest wing root bending moment, and the taxi loads expose the wing lower surface covers to compression. Cross-sectional dimensions established in the process of strength sizing include thicknesses of the face sheets of the wing cover sandwich panels and thicknesses of the rib and spar webs. This design constitutes a starting point for subsequent flutter resizing. A typical distribution of wing cover thicknesses obtained in this manner can be found in Fig. 12 of Ref. 5.

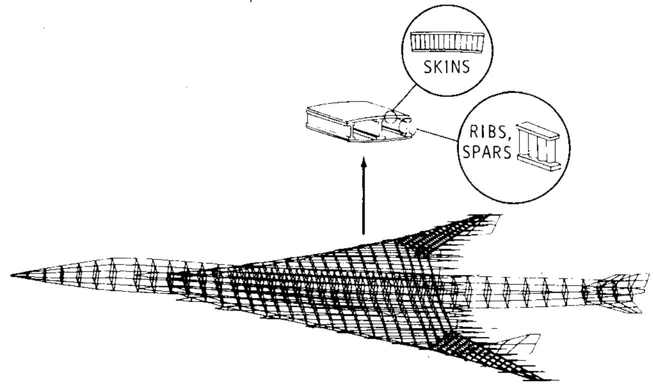

Fig. 1 Finite-element model with details of the wing construction.

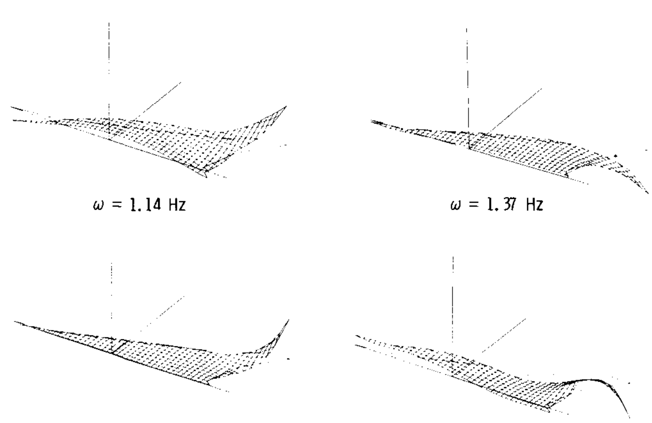

Fig. 2 The lowest elastic natural vibration modes for the strength-sized airframe.

Dynamic Behavior

Because of its large size and flexible wings, the airframe exhibits a complex vibratory behavior. This behavior is shown in plots of the wing planform for the four lowest vibration modes (Fig. 2). Although the flexible wing tip contributes most heavily to the modal deformation, there is considerable coupling with the inboard delta-like portion of the wing and with the fuselage, and a pronounced chordwise bending deformation which distinguishes the arrow-wing's behavior from that of a conventional high-aspect-ratio wing.

All flutter analyses during the design process and for final designs are performed for the aircraft with a light fuel condition using only the symmetric vibration modes. In previous studies it has been shown that the light fuel case is critical and that the flutter modes calculated using asymmetric vibration modes are very similar to the symmetric modes. However,

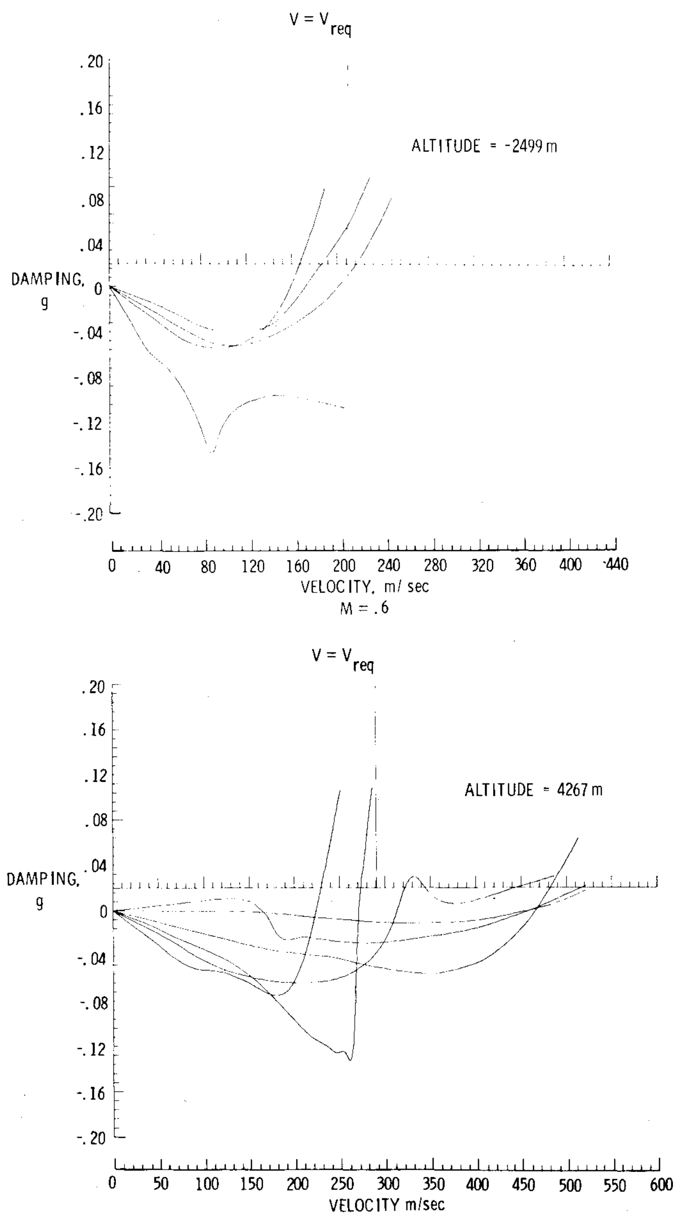

Fig. 3 *V-g* plots for the strength-sized aircraft.

both additional fuel conditions and asymmetric flutter modes could be handled by the flutter resizing procedure used in this study. Figure 3 shows the results of the flutter analysis for the airframe after a strength sizing has been performed. It can be seen that the aircraft is severely flutter deficient relative to the required flutter speeds at both Mach 0.6 and 0.9. Previous studies have shown that these are the critical Mach numbers for this aircraft and both are considered in the flutter resizing procedure. The altitudes at which the flutter analyses are performed for these two Mach numbers were selected to produce the required dynamic pressures to satisfy the necessary margins on flutter speed relative to the flight envelope. They are −2499 and 4267 m, respectively, for the two Mach numbers. The horizontal axes in the *V-g* plots of Fig. 3 are located at $g = 0.02$, which is the value of structural damping assumed for the airframe. It is important to note that three different flutter modes are close to the required flutter speed at both Mach 0.6 and 0.9. Thus it is important for this application that the flutter resizing procedure be able to handle multiple modes.

Description of the Flutter Resizing Method

The resizing method discussed here is essentially that of Ref. 3 with several modifications. The principal ingredients of the method are an approximate flutter analysis using reduced basis techniques, the use of a general purpose optimizer based on nonlinear mathematical programming, a continuous flutter constraint formulation, and a strategy for periodically recalculating the natural vibration modes by solving the global eigenvalue problem. These topics are discussed in the following sections and a summary of the steps in the resizing procedure is presented.

Reducing the Size of the Flutter Analysis Problem

To reduce the cost of the repetitive vibration analyses of the airframe, a method was proposed in Ref. 3 which is based on using an approximate analysis to calculate the set of vibration modes for use in the flutter calculations. This approximate analysis is based on a modal approach (similar to that used in the solution of the flutter eigenvalue problem) where the vibration modes for the modified structure are represented by a linear combination of the natural modes from a previous solution of the global, finite-element equations. The participation factors in this linear combination are determined by solving a small vibration problem of the order of the number of modes in the linear combination. This number of modes used as approximation functions is larger than the number of modes used in reducing the flutter eigenvalue problem, but is much smaller than the number of degrees of freedom in the finite-element model. A much larger number of generalized degrees of freedom can be used in the approximate vibration problem compared with the flutter eigenvalue problem because the vibration problem is solved only *once* for each modified structure. This approximate technique drastically cuts the cost of the vibration analysis and provides a good set of approximate modes for the flutter analysis. As the structure changes significantly from the design produced when the global vibration problem was previously solved, the accuracy of the approximate modes may be unacceptable and a new set of modes must be calculated from the global problem; however, this is required only a few times for a complete design run.

The first step in the approximate flutter analysis is the solution of the global vibration problem

$$[K][\Delta] = \Omega^2 [M][\Delta] \quad (1)$$

for the set of m_1 lowest modes and frequencies. The matrices $[K]$, $[M]$, and $[\Delta]$ are of the order of the total number of degrees of freedom in the finite-element model. The set of lowest m_1 vibration modes is denoted $[\phi]$. Note that the value of m_1 is significantly larger than the number of modes to be used in solving the flutter eigenvalue problem, m_2. Employing the transformation

$$[\Delta] = [\phi][\delta] \quad (2)$$

the generalized stiffness, mass, and aerodynamic force matrices

$$[\bar{K}] = [\phi]^T [K][\phi]$$
$$[\bar{M}] = [\phi]^T [M][\phi]$$
$$[\bar{A}] = [\phi]^T [A][\phi] \quad (3)$$

and derivatives of the stiffness and mass matrices with respect to the design variables

$$\left.\begin{aligned}[\bar{K}_i] &= [\phi]^T [\partial K/\partial v_i][\phi] \\ [\bar{M}_i] &= [\phi]^T [\partial M/\partial v_i][\phi]\end{aligned}\right\} i = 1, n \quad (4)$$

are formed. The matrices of aerodynamic influence coefficients, $[A]$ in Eq. (3), can be calculated for the different Mach numbers and reduced frequencies using any appropriate linear, unsteady aerodynamics theory. The generalized derivative matrices $[\bar{K}_i]$ and $[\bar{M}_i]$ are formed so that generalized stiffness and mass matrices for the modified structure can be formed exactly and quickly by linear Taylor expansion. The generalized matrices can be formed exactly by Taylor expansion because the membrane finite elements used are linear functions of the design variables. For given values of the design variables representing a modified structure designated by j, the reduced approximate vibration problem is

$$[\bar{K}_j][\delta] = \Omega_j^2 [M_j][\delta] \quad (5)$$

Since this eigenvalue problem is only of order m_1, the lowest m_2 modes can be calculated with very small cost. This set of m_2, lowest approximate vibration modes is denoted $[q]$. Employing the transformation

$$[\delta] = [q][u] \quad (6)$$

the generalized stiffness mass, and aerodynamic force matrices of order m_2

$$[\bar{\bar{K}}_j] = [q]^T [\bar{K}_j][q]$$
$$[\bar{\bar{M}}_j] = [q]^T [\bar{M}_j][q]$$
$$[\bar{\bar{A}}_j] = [q]^T [\bar{A}][q] \quad (7)$$

are computed for the modified structure. The complex flutter eigenvalue problem

$$\{\omega^2 [\bar{\bar{M}}_j] + (1 + ig)[\bar{\bar{K}}_j] + q[\bar{\bar{A}}_j]\}[u] = [0] \quad (8)$$

which is of order m_2 can be solved to give values of velocity and damping for the reduced frequencies and the flutter modes used in calculating the constraints.

The operations indicated in Eqs. (5-8) are performed for every modified structure in the design process. However, these operations are relatively inexpensive. The operations indicated in Eqs. (1-4) are relatively costly but are performed only a few times during a design run.

Formulation of the Flutter Constraints

The flutter constraint formulations of Refs. 2 and 3 are designed to prevent any flutter modes from violating the flutter requirements at any point in the design process. As the airframe is resized, it is highly possible that flutter modes which were not initially critical will become critical. These

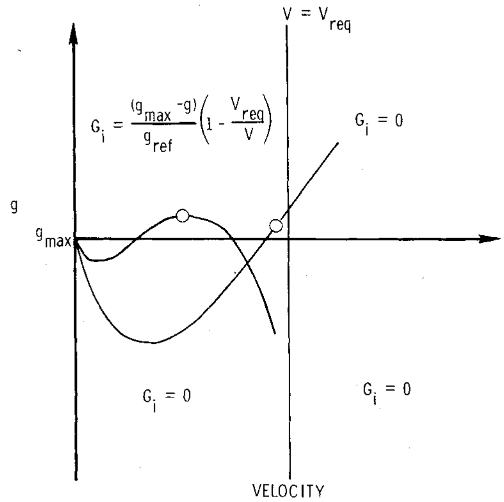

Fig. 4 Definition of the flutter constraint on a typical V-g plot.

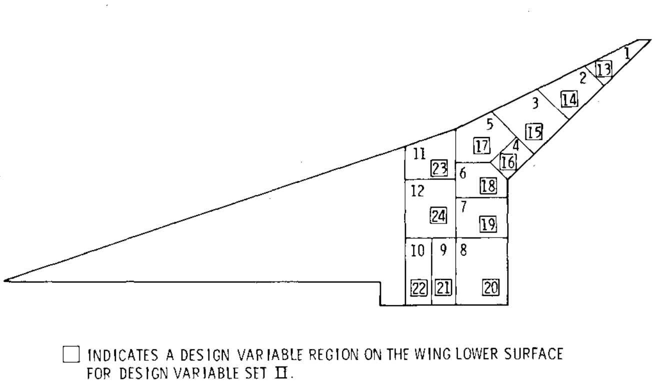

Fig. 5 Cover panel thickness regions controlled by design variables.

flutter modes initially may have crossed the $g=g_{max}$ axis at speeds higher than the required speed or may not have crossed at all (this is the so-called "hump" mode). The constraint formulation of Refs. 2 and 3 considers both cases.

In this study a modification was made to the constraint formulation of Ref. 3 because of the different optimization algorithm used. A general purpose optimizer, denoted CONMIN (Ref. 7), based on a feasible directions method was employed rather than the penalty function method of Ref. 3. In order to permit deletion of unimportant constraints during the design process and satisfy the requirements of CONMIN regarding the ordering of constraints passed to it, a cumulative constraint formulation was used.

The values of the constraint G_i in the four regions of the V-g diagram are shown in Fig. 5; a value of $G_i > 0$ indicates violation of the constraint. The cumulative constraint is defined as

$$G_{cum} = \sum_i G_i^2 \tag{9}$$

During design, V-g points for a number of reduced frequencies (~ 100 for the studies reported herein) on all flutter modes are calculated, and the constraints associated with these points are summed in Eq. (9). The circles in Fig. 4 indicate typical V-g points at values of the reduced frequency that contribute to the constraint. Constraints for other Mach numbers or altitudes being considered are also summed in Eq. (9). Thus the complete flutter behavior of the aircraft is represented by the single constraint, Eq. (9).

Strategy for Updating the Vibration Modes

As the design changes significantly from that when the global vibration problem was previously solved, the approximate vibration analysis may become unacceptably inaccurate. The global problem (order m_0) is then re-solved for this new, modified structure. The difficulty is selecting the appropriate criterion for returning to the global problem.

In Ref. 3, changes in the lowest natural vibration frequency are used in a criterion to determine when to recalculate the complete set of vibration modes. When the approximate frequency for the modified structure differs from the lowest frequency calculated in the last global analysis, a new set of exact vibration modes and frequencies are calculated. An advantage of this criterion is that it attempts to directly measure differences in the vibration behavior between the structure for which exact modes were calculated and the modified structure. A disadvantage is that the first vibration mode and frequency may not be one of the dominant ones in the flutter analysis; this is the case for certain flutter conditions of the supersonic transport model.

In this application, the indirect approach of controlling the accuracy of the approximate analysis by specifying "move limits" on the design variables is used. This approach was used successfully in Ref. 8 and has the advantage of being easy to implement. With move limits the optimizer is simply not allowed to change the design variables by more than a specified percentage until a new solution of the global vibration problem is performed. Since a single design variable controls a number of individual elements and since the design variables are panel thickness additions, the move limits are related to the thickest panel in each design variable region. The upper and lower values for a particular design variable are a certain percentage above and below the thickness of this specified panel. A minimum gage requirement of zero is also placed on the lower value, which specifies that no reductions of the thicknesses in the strength-sized design are allowed. These values are supplied to the optimizer, which performs a complete minimization based on these bounds. The process of solving the global vibration problem, prescribing move limits, and performing a complete minimization of the mass is called a *cycle*.

As the design procedure moves from cycle to cycle, the move limit percentage is reduced by a prescribed factor. The approach is to start with relatively liberal move limits and then tighten the range of the approximate analysis near the final design.

Summary of Steps in the Flutter Resizing Procedure

1) Select the group of structural parameters controlled by each design variable. In the application reported herein, the design procedure is being applied to a structure already sized for strength considerations and the design variables are thickness additions to cover panels on the upper and lower surfaces of the wing. To reduce the number of the design variables considered, the thickness additions to a number of adjacent finite elements are controlled by a single design variable.

2) Compute the derivatives of the mass with respect to the design variables. Since the design variables are thicknesses, the derivatives are independent of the values of the design variables and are computed only once.

3) Form the mode independent aerodynamic force coefficients at the different Mach numbers being considered for a specific set of reduced frequencies for the important lifting surfaces (both the wing and tail are considered in this study). These coefficients depend only on Mach number, reduced frequency, and surface geometry, which are not changed during redesign. Thus these coefficients are calculated only once. The aerodynamic calculations are based on the kernel function method for subsonic flow and the computer implementation described in Ref. 9.

4) Form the global finite-element stiffness and mass matrices based on the current values of the design variables.

5) From the global equations, calculate a set of m_1 natural vibration modes and frequencies. The number of modes m_1

should be significantly larger than the number of modes finally used in the flutter calculations.

6) Form the generalized stiffness and mass matrices of order m_l [Eq. (3)] and their derivatives with respect to the design variables [Eq. (4)].

7) Form the matrix of generalized aerodynamic forces using the set of m_l natural vibration modes. The modal deflections at the structural mode points are interpolated using spline functions to the aerodynamic collocation points. This matrix is denoted $[\tilde{A}]$ [Eq. (3)].

8) Based on the current values of the design variables and the move limit factor, determine the upper and lower move limits for each design variable.

9) For given values of the design variables, v_i, compute the mass penalty and the generalized stiffness and mass matrices by Taylor expansion [Eq. (5)].

10) Solve the reduced eigenvalue problem of order m_l [Eq. (5)] for a set of m_2 vibration modes and frequencies $(m_2 < m_l)$. These are *approximations* to the lowest m_2 vibration modes for the *modified* structure.

11) Compute generalized stiffness, mass, and aerodynamic matrices of order m_2 [Eq. (7)]. Note that $[\bar{K}]$ and $[\bar{M}]$ are always diagonal and this fact can be exploited in the flutter eigensolution method.

12) Solve the complex flutter eigenvalue problem of order m_2 [Eq. (8)] at the Mach numbers and altitudes being considered. Constraints and possibly derivatives of the constraints with respect to the design variables (depending on the request by the optimizer) are calculated for all critical points on the *V-g* diagram.

13) Execute the optimizer, which determines a new set of design variables and requests an analysis for this design or indicates that a minimum mass has been found. If a minimum has not been found, go back to step 9 and continue; otherwise, go to step 14.

14) If the maximum number of cycles has not been reached, go to step 4 to update the m_l vibration mode set by solving the global equations. At this time the factor specifying the move limits on the design variables is reduced by the specified percentage.

15) Perform a calculation of vibration modes and flutter speeds for the final design to insure that the flutter requirements are met.

Computer Implementation of the Resizing Procedure

The resizing procedure is implemented within the EAL (Engineering Analysis Language) system (Ref. 10), which is a derivative of the SPAR structural analysis system (Ref. 11). In addition, computational modules from the PARS flutter resizing procedure (Refs. 3 and 12) and the general purpose optimizer CONMIN (Ref. 7) were added to the EAL system.

Application and Results

A number of numerical studies have been performed to demonstrate the application of the previously described flutter resizing method to a supersonic transport configuration. Mass penalties, values of the design variables, and *V-g* diagrams for the final designs are presented to characterize the flutter-free aircraft. Design iteration histories for the mass penalty are presented to show the behavior of the method.

Determination of the Number of Modes

The two key parameters of the resizing method which must be selected are 1) m_2, the number of modes used in the *V-g* flutter analysis, and 2) m_l, the number of modes used in the approximate vibration analysis. A convergence study was performed using the strength-sized aircraft to determine how the number of modes used affects the calculated flutter speeds. After considering the computational cost of calculating the flutter constraints during the design process, the value of $m_2 = 12$ was selected, which gives flutter speeds at both Mach 0.6 and 0.9 which are about 5% high. To counteract this unconservative analysis, a modification factor, f_v is used to increase the required flutter speed V_{req} used in calculating the flutter constraints. Even though the error between the 12 mode flutter solution and the converged solution is not constant during the design process, the initial error provides a guideline for selecting f_v.

The constant m_l should be considerably larger than m_2 but small enough so that the calculation of m_l vibration modes from the global equations is computationally practical. Another factor which limits the size of m_l is the cost of computing the generalized matrices [operations indicated in Eqs. (3) and (4)]. Although m_l is also the order of the reduced free vibration problem [Eq. (5)], the cost of solving this eigenproblem is negligible relative to the above operations. Based on these considerations m_l was selected to be 24. This number of modes is also used in the flutter analysis of the final design, which is performed only once. For this application, the computational cost reductions are achieved specifically by reducing the dimensionality of the problem from 2141 degrees of freedom in the global equations, to 24 degrees of freedom in the reduced vibration problem, to 12 degrees of freedom in the flutter eigenvalue problem.

Definition of the Design Variables

The flutter resizing procedure begins from a design sized for strength considerations in which the thickness of each individual finite element (both membrane wing skins and shear panel spar and rib webs) was controlled by a design variable. Since this large number of design variables is not practical in the flutter resizing procedure, only the wing cover skin thicknesses are changed during flutter resizing. A number of finite elements are controlled by a single design variable, with each design variable representing a thickness addition to all elements in that particular region.

Two different sets of design variable regions were considered in this study; both sets are shown in Fig. 5. In set I, each of the 12 design variables controls skin thicknesses on both the upper and lower wing surfaces. In set II, the skins on the lower wing surface are controlled by 12 additional design variables. The layouts of the regions on upper and lower surfaces, as can be seen in Fig. 5, are identical. Set II was considered, since in the initial, strength-sized design, the upper and lower wing cover panels are not symmetric. Therefore, if the optimizer had the freedom to increase the skin thicknesses of upper and lower panels independently, a more symmetric design might be achieved which should be more efficient for bending stiffness.

Number of Design Cycles

Since each cycle requires a new solution of the global eigenvalue problem, it is important to keep the number of cycles small. Therefore two of the four design cases were performed using only a single cycle. The modification factor f_v was used to account for any discrepancies between the approximate analysis in the design process and the final analysis. Some numerical experimentation was required to select f_v, but after the appropriate value was determined, correlation between the approximate flutter speeds and those from the final analysis was excellent. The other two design cases had five resizing cycles with controlled move limits.

Final Resized, Flutter-Free Designs

The results of four design cases are presented in this section. The four cases are A) resizing with the 12 design variable set I and only a single cycle; B) resizing with the 24 design variable set II and only a single cycle; C) resizing with the 12 design variable set and five cycles; and D) resizing with the 24 design variable set and five cycles.

The values of the design variables and the mass penalties for each of the four designs are shown in Fig. 6. The mass

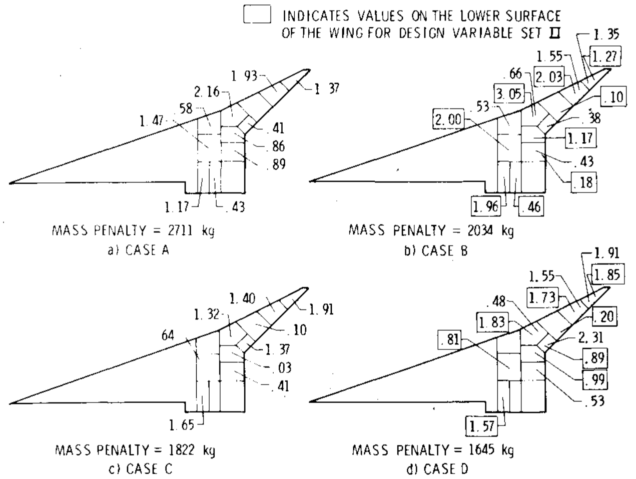

Fig. 6 Final design variable values for the four cases. Values are sums of upper and lower sandwich face sheet thickness additions in mm.

Table 1 Comparison between the lowest elastic natural frequencies (Hz) of the strength-sized and flutter-resized (case D) aircraft

Strength-sized	Case D	Change, %
1.136	1.148	1.0
1.372	1.378	0.4
2.146	2.269	5.4
2.723	2.780	2.1
3.272	3.460	5.4
3.813	4.973	4.0
4.453	4.997	10.9
5.248	5.276	0.5
5.624	5.652	0.5

penalty represents the amount of material added to the total airframe to prevent flutter. In all four designs the upper and lower skins in the tip portion of the wing have been thickened considerably. Material added in this area can act both as a "balancing mass" and to stiffen this flexible tip. Since this portion of the wing is nearly symmetric after strength-sizing, nearly equal additions were made to upper and lower skins. Large thickness additions have also been made between the tip and delta portions of the wing, the region controlled by design variables 5 and 17. In this region the upper and lower wing skins are highly asymmetric after strength-sizing. For design cases B and D, considerably more material is added to the lower skin to produce a more symmetric design. The wing region controlled by design variables 10 and 22 is consistently thickened in all flutter-resized designs even though it is a considerable distance from the more flexible area of the wing. However, the wing carry-through structure is located near this region. A structural modification of this type might easily be overlooked using intuitive techniques for resizing the wing to prevent flutter.

Design case A has by far the largest mass penalty but it was produced with the crudest analysis (a single design cycle) and considered only 12 design variables. Improving the design procedure by including more refined analyses (cases C and D) or additional design variables (cases B and D) lowers the mass penalty. The lightest flutter-free design, case D, has a mass penalty which is 7% of the wing structural mass and 6.5% of the aircraft's payload.

Table 1 compares the values of the lowest natural vibration frequencies of the strength-sized airframe with those of the flutter-resized airframe. Even though 20% increases in the flutter speeds have resulted from resizing, the changes in the vibration frequencies are fairly small. The change in the first natural frequency, which is used as a mode update criterion in Ref. 3, is only 1%.

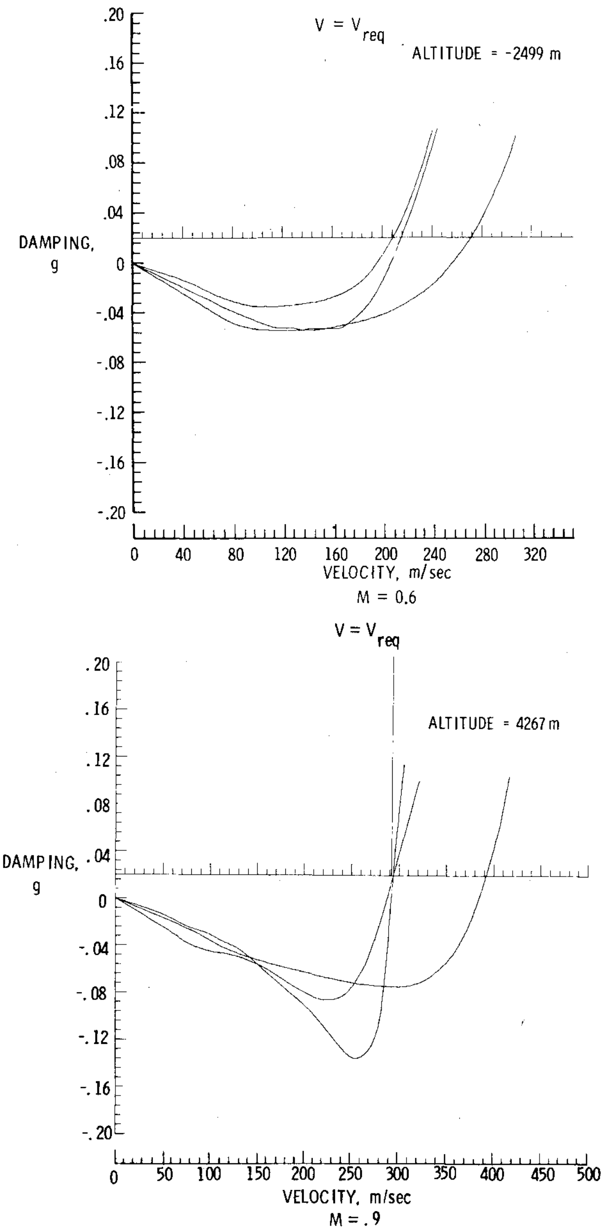

Fig. 7 *V-g* plots for the aircraft resized to meet flutter requirements (case D).

Figure 7 shows the *V-g* diagrams for the flutter-resized design (case D) at Mach 0.6 and 0.9. As mentioned previously, two flutter modes are important at both Mach numbers for the strength-sized design. The resizing procedure has driven the design in a direction such that at both Mach numbers, both modes are nearly critical. This is consistent with the intuitive notion that a minimum mass design is characterized by simultaneous failure in multiple modes. It also clearly demonstrates that the resizing procedure can effectively account for multiple critical flutter modes.

To gain additional insight into the behavior of the flutter-resizing process, design histories of the mass penalty for cases B and D are shown in Fig. 8. The mass penalties are plotted vs the iteration number, where an iteration in the feasible directions algorithm is defined as a single minimization in a specified direction in the design space. With only one design cycle (case B), the design variables have no move limits and the optimizer drives the design quickly to a high mass in order to produce an acceptable (flutter-free) design. It then quickly reduces the mass to achieve the minimum mass design for this case. With five design cycles and move limits on the design variables (case D), the optimizer is not allowed to make these very large changes in the structure early in the design process.

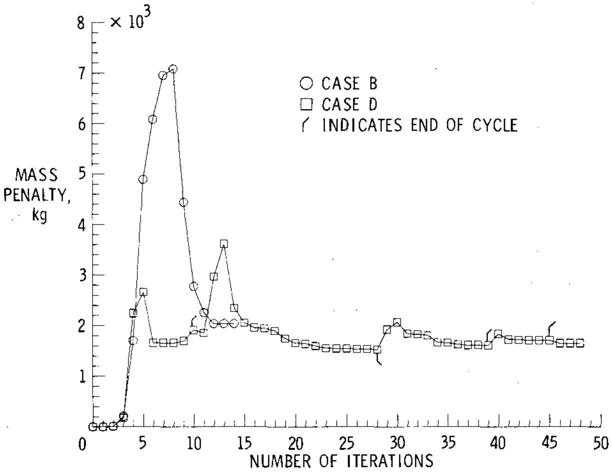

Fig. 8 Design iteration histories for the mass penalty.

Concluding Remarks

A procedure for sizing an airframe for flutter-free performance has been demonstrated on a large, flexible supersonic transport aircraft. The procedure is based on using reduced basis or modal techniques for reducing the computational cost of performing flutter analyses. This supersonic transport aircraft exhibits complex dynamic behavior, has a well-known flutter problem and requires a large finite-element model to predict vibratory and flutter response; thus resizing this airframe to alleviate flutter is a very difficult problem.

The following conclusions were drawn from the numerical design studies:

1) Flutter-free designs of the aircraft with small mass penalties have been produced. For case D, the mass penalty is 7% of the wing structural mass and 6.5% of the aircraft's payload.

2) The two-level modal analysis drastically reduces the cost of the repetitive flutter calculations and makes resizing using the complex finite element model feasible.

3) Execution of the resizing procedure with only a single solution of the finite-element vibration problem and using a modification factor on the required flutter speed produced a design with a moderately small mass penalty. For case B, the mass penalty is 9% of the wing structural mass and 8% of the payload.

4) The procedure can effectively handle multiple flutter modes as evidenced by the final designs having two modes simultaneously critical.

5) In view of the ability of the resizing procedure to consider the complex dynamic behavior of this airframe and produce a flutter-free design with a small mass penalty, the method can probably be used for many other aircraft.

References

[1] Stroud, W. J., "Automated Structural Design with Aeroelastic Constraints: A Review and Assessment of the State of the Art," edited by L. A. Schmit Jr., paper presented at the ASME Symposium on Structural Optimization, AMD, Vol. 7, ASME, 1974, pp. 77-118.

[2] McCullers, L.A. and Lynch, R.W., "Dynamic Characteristics of Advanced Filamentary Composite Structures, Vol. II—Aeroelastic Synthesis Procedure Development," AFFDL-TR-73-111, Sept. 1974.

[3] Haftka, R.T. and Prasad, B., "Programs for Analysis and Resizing of Complex Structures," paper presented at the Symposium on Future Trends in Computerized Structural Analysis and Synthesis, Wash., D.C., Oct. 30-Nov. 1, 1978; see also *Trends in Computerized Structural Analysis and Synthesis,* Pergamon Press, New York, 1978, pp. 323-330.

[4] Hogley, J.R. and Weatherill, W.H., "SST Technology Program—Phase II: A Flutter Analysis Program to Achieve an Optimized Structure for a Supersonic Transport Airplane," FAA-SS-73-13, Feb. 1974.

[5] Sobieszczanski-Sobieski, J., Gross, D., Kurtze, W., Newsom, J., Wrenn, G., and Greene, W., "Supersonic Cruise Research Aircraft Structural Studies: Methods and Results," paper presented at the 1979 Supersonic Cruise Research Conference, NASA LaRC, Hampton, Va., Nov. 1979, NASA CP-2108, pp. 617-656.

[6] Sobieszczanski, J., "Sizing of Complex Structures by the Integration of Several Optimal Design Algorithms," AGARD Lecture Series No. 70 on Structural Optimization, AGARD-LS-70, Sept. 1974.

[7] Vanderplaats, G.N., "CONMIN-A Fortran Program for Constrained Function Minimization," User's Manual, NASA TM X-62282, 1973.

[8] Stroud, W.J., Agranoff, N., and Anderson, M.S., "Minimum-Mass Design of Filamentary Composite Panels Under Combined Loads: Design Procedure Based on a Rigorous Buckling Analysis," NASA TN D-8417, July 1977.

[9] Desmarais, R.N. and Bennett, R.M., "User's Guide for a Modular Flutter Analysis Software System (FAST Version 1.0)," NASA TM-78720, May 1978.

[10] Whetstone, W.D., "Engineering Data Management and Structure of Program Functions in New Techniques in Structural Analysis by Computer (compiled by R.J. Melosh and M. Salana)," preprint 3601 presented at the ASCE Convention and Exposition, Boston, Mass., 1979.

[11] Whetstone, W.D., "SPAR Structural Analysis System Reference Manual—System Level 13A, Vol. I-Program Execution," NASA CR-148970-1, 1978.

[12] Haftka, R.T., Prasad, B., and Tsach, U., "PARS—Programs for Analysis and Resizing of Structures—User Manual," NASA CR-159007, April 1979.